engineering proceedings

MDPI

Proceeding Paper

Advanced Receiver Autonomous Integrity Monitoring (ARAIM) for Unmanned Aerial Vehicles †

Merle Snijders [1,*], Heiko Engwerda [1], Javier Fidalgo [2,*], Enrique Domínguez [2], Ginés Moreno [2], Fulgencio Buendía [2], Joao Pedro Duque [2], Jorge Martínez [2], Ilaria Martini [3], Matteo Sgammini [3] and Juan Pablo Boyero [4]

[1] Department of Aerospace Systems, Royal Netherlands Aerospace Centre (NLR), 1059 CM Amsterdam, The Netherlands
[2] NUSP Business Unit, GMV, 28760 Tres Cantos, Madrid, Spain
[3] Joint Research Centre (JRC), European Commission, 21027 Ispra, Italy
[4] Defence Industry and Space (DEFIS), European Commission, Rue de la Loi 130/Wetstraat 130, 1049 Brussel, Belgium; juan-pablo.boyero@ec.europa.eu
* Correspondence: merle.snijders@nlr.nl (M.S.); jfidalgo@gmv.com (J.F.)
† Presented at the European Navigation Conference 2023, Noordwijk, The Netherlands, 31 May–2 June 2023.

Abstract: Advanced Receiver Autonomous Integrity Monitoring (ARAIM) is an evolution of the currently used aviation-focused Global Navigation Satellite System integrity service, Receiver Autonomous Integrity Monitoring (RAIM). Where RAIM supports only lateral navigation, with its adaptations including multiple frequencies and constellations, and with the use of Integrity Support Messages (ISMs), ARAIM also supports vertical guidance. Although these techniques were designed to serve the aviation community, ARAIM could be used in a wide range of applications, especially safety-critical applications. With further evolutions, ARAIM could also be extended to cover more demanding applications in various sectors. This work reports the outcomes of the study of the applicability of ARAIM for the Unmanned Aerial Vehicle (UAV) sector.

Keywords: integrity; ARAIM; GNSS; UAV; HAS; sensor fusion

Citation: Snijders, M.; Engwerda, H.; Fidalgo, J.; Domínguez, E.; Moreno, G.; Buendía, F.; Duque, J.P.; Martínez, J.; Martini, I.; Sgammini, M.; et al. Advanced Receiver Autonomous Integrity Monitoring (ARAIM) for Unmanned Aerial Vehicles. *Eng. Proc.* **2023**, *54*, 46. https://doi.org/10.3390/ENC2023-15435

Academic Editors: Tom Willems and Okko Bleeker

Published: 29 October 2023

1. Introduction

The UAV sector represents a rapidly growing market; according to different reports, its value will triple between 2020 and 2030 [1]. The navigation system within the majority of these vehicles relies on GNSS as a primary means of positioning. Many operations are expected to be conducted in densely populated urban environments, which means that the requirements of navigation accuracy and especially integrity are stringent [2].

ARAIM is a promising integrity technique which could meet the requirements of the UAV sector. As shown in the ARAIMTOO project [3], the ARAIM concept for aviation can already meet the requirements of some non-aviation applications, in particular those operated in open-sky conditions. For the most demanding applications, operated in non-open sky conditions or with requirements more stringent than those in aviation, the evolution of the ARAIM concept is needed.

For the UAV sector, the following high-level ARAIM evolutions have been investigated within the ARAIMTOO project: the combination of dual constellation (GPS + Galileo) multi-frequency GNSS signals and Precise Point Positioning (PPP) techniques with an integrity algorithm at user level as ARAIM with hybridization with IMU, which could allow it to cope with harsh environments typical of urban areas and the stringent accuracy and integrity requirements of UAVs in urban environments.

To prove the concept of the ARAIM evolutions, an experiment was conducted based on the adapted Matlab Algorithm Availability Simulation Tool (MAAST), developed by Stanford [4]. In this adaptation, the ARAIM algorithms implemented are aligned with the

ARAIM ADD version 4.0, as implemented in the tool, and the proposed ARAIM evolutions have been prototyped.

Secondly, a MATLAB post-processing tool was developed to analyse collected flight data. With the use of this data, the fault detection and exclusion (FDE) and protection levels (PLs) were analyzed for real-life user scenarios.

2. Architecture of the Algorithm Evolution

The proposed evolution of the ARAIM algorithm for UAV implementations consists of the augmentation and extension of the GNSS signal by means of the recently rolled-out High Accuracy Service (HAS) as well as hybridization with an Inertial Measurement Unit (IMU). This combination shall result in high-accuracy PVT (position, velocity and time) solutions in combination with tight integrity budgets associated with the demanding urban user environment.

An overview of the implementation of this architecture is shown in Figure 1. The measurements and information are retrieved as displayed on the left side. The core of the ARAIM evolution is a Kalman filter followed sequentially by the ARAIM (snapshot) algorithm. The filter is fed with IMU measurements: accelerations and angular rates applicable to the inertial frame. As this frame has a certain offset in both its position and attitude from the GNSS antenna phase center, a set of corrections has to be provided to the filter as well. The second set of measurements is obtained from the GNSS receiver, in the figure displayed as the Multi-Frequency Multi-Constellation Galileo and GPS data. This data is augmented by the PPP corrections through the HAS. In order to apply this model, the ionospheric free combinations have to be determined based on the multi-frequency signals. Both the carrier phase and code phase measurements are implemented, with which the filter can model the state variables. The additional error states, in combination with the IMU error model and performance specifications, are integrated in the Kalman filter. Within the filter, the variances and error states are monitored and evaluated in order to provide a first FDE attempt, referred to as the FDE_{KALMAN}. Based on the increased navigation performance of the hybridization scheme, faulty satellites can be detected and excluded. The set of remaining satellites is then communicated to the ARAIM algorithm, as the 'all-in-view' solution. Other data that need to be transmitted from the filter to the ARAIM algorithm are the carrier phase measurements corrected for atmospheric disturbances and the solved ambiguities. As the ARAIM error model requires variances to calculate the PL, the KF variances are also shared, including the ambiguities and atmospheric variances. Furthermore, based on the external (sensor) input or from a monitoring scheme based on the state prediction residuals, the variance of the error due to the user environment can be estimated. Based on the ISM data fed to the ARAIM algorithm, the subsets of to-be-monitored solutions can be obtained. The same strategy to determine the PL is followed as in the legacy ARAIM algorithm. FDE_{ARAIM} can still be performed, although the effects are negligible, as the PPP KF already implements an FDE_{ARAIM} algorithm based on the hybridized solution.

In parallel to the ARAIM algorithm, the navigation solution can be propagated relying on the higher-frequency IMU data. Based on the IMU performance specifications, the PL can be inflated over time to account for drift. Careful consideration is required here, as long periods without GNSS cause an exponential drift. For shorter intervals, the behaviour can be expected to be close to linear.

Once the GNSS and a new ARAIM-calculated PL become available, the propagated PL and new PL can be compared and a new PL can be selected. This approach can be helpful in bridging the GNSS data gaps and cases where PPP convergence is lost.

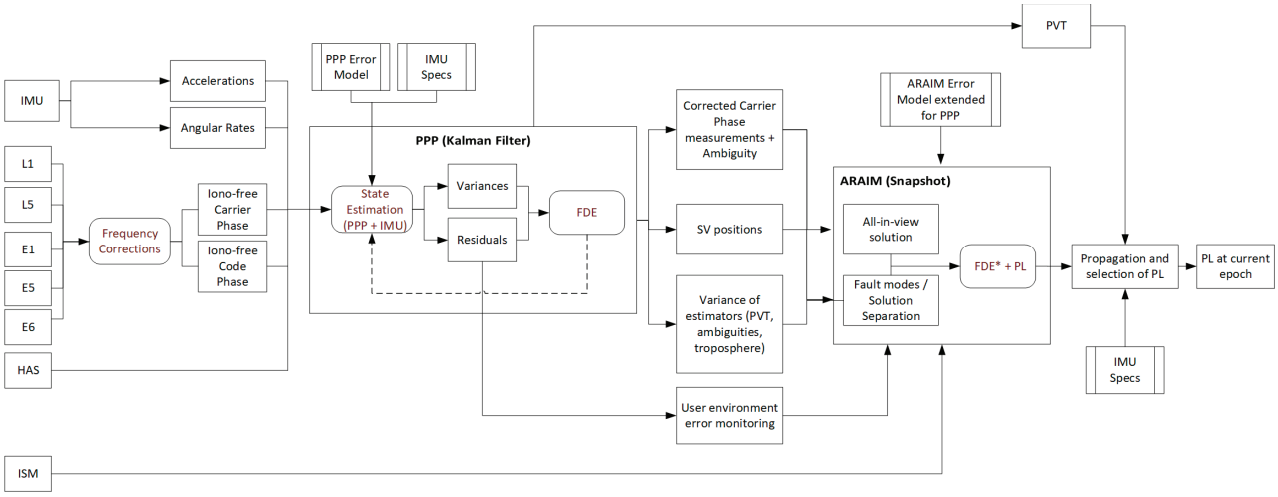

Figure 1. ARAIM evolution architecture for UAV applications. Note that the FDE* in the snapshot ARAIM block is different from the legacy FDE implementation.

3. Test Cases

By means of a series of test cases, the performance and behaviour of the ARAIM evolution can be tested. In this section, two test cases will be evaluated; first, a simulated set where spatial and temporal variation are covered, and a second set, where actual flight data is evaluated with feared events added.

3.1. Test Case 1

In this test case, service volume simulations using the modified MAAST code are performed. With such simulations, the global protection levels and availability performance are assessed for the ARAIM evolution for UAVs. This evolution implements both PPP through the HAS as well as IMU through a hybridized solution. In order to simulate the effects of PPP, an improved set of parameters has been supplied to the simulator:

- P_{sat}: the prior probability of a satellite fault, reduced to account for the monitoring efforts in supplying the PPP correction data.
- P_{const}: the prior probability of a constellation-wide fault, reduced to account for the monitoring efforts in supplying the PPP correction data.
- B_{nom}: the effects of the nominal bias are compensated with the PPP input data (precise data).
- URA: the PPP corrections will provide a better ranging accuracy. Note that a reduced overbounding distribution results in an increased probability of an error being considered a fault, which is assumed to be covered by the prior probability of a satellite fault.

The HAS service does not provide integrity monitoring commitment. Therefore, two different P_{sat} and P_{const} values, the original values and improved values, are simulated. In this way, the potential improvement due to HAS can be shown. Furthermore, the error budget is augmented with the following parameters:

- σ_{IMU}: the user error budget must be extended with the errors due to the propagation with IMU measurements.
- σnonlos: in an urban environment, this sigma bounds the errors due to non-line-of-sight signals not being detected by the FDE and entering the solution.
- $P_{FDE\text{-}MD}$: the probability of missed detection by the FDE algorithm is introduced to represent the occurrences where a non-line-of-sight signal is used by the receiver, resulting in an increased user variance, as explained in the previous bullet point.
- $P_{cycleslip}$: the probability of a non-detected cycle slip is added to the prior fault probability of the satellite.

3.2. Test Case 2

For this test case, the FDE capability of the ARAIM evolution for the UAV sector is central. In order to test its ability to exclude erroneous measurements, a set of input data should be used that includes such events. For this purpose, UAV flight data (IMU + dual antenna GNSS) is used with a trajectory following waypoints and manual flights, without any masking or interference, as the input data. A set of feared events is simulated by adding observation errors to this input data. These events mimic the conditions of the urban environment, and provide a robustness check against feared events such as ionospheric scintillation. These events are introduced in five specific intervals, as shown in Table 1.

Table 1. Table with inserted feared events.

Feared Event	Value/Description	Comments and Justification (If Needed)	Time Window
Slowly accumulating fault	Single satellite fault 10 cm per second increment	A slowly increasing pseudorange and phase measurement is modified in the observation file.	12:17:35–12:18:00
Multipath	Pseudorange: 1–5 m, phase measurement: negative of multipath pseudorange effect converted to cycles, 10–16.5 dB signal reduction	Multipath is applied to both pseudorange and phase measurement, for all applied frequencies and constellations. The exact value is drawn from a random uniform distribution. Reference values taken from [5].	12:22:00–12:22:30
Blanking	Multiple satellites unavailable	Based on the service volume simulations conducted, the difference between open-sky and urban environments can result in a loss of 6 visible satellites when utilizing two constellations. These satellites are chosen from the lowest elevation PRNs visible.	12:27:00–12:28:00
Non-line-of-sight	5–10 m pseudorange, 10–16.5 dB signal reduction	Values are chosen to represent non-line-of-sight signals arriving at the receiver while the direct path is obstructed. The exact value is drawn from a random uniform distribution. Reference values are taken from [6].	12:31:00–12:31:30
Multipath and blanking combined	1–5 m pseudorange, 10–16.5 dB signal reduction.Multiple satellites unavailable	This scenario is a combination of the multipath and blanking (4 satellites, based on elevation) described above.	12:33:00–12:33:30

In order to verify the ability of the FDE algorithms to mitigate feared events in this scenario, ideally, a reference truth trajectory is available that is not correlated with the GNSS errors. As such a dataset was not available, the approach is taken to introduce simulated feared events to a dataset where faults are introduced during the campaign. The open sky dataset is best suited for this approach.

4. Experimentation and Simulation Results

4.1. Test Case 1

4.1.1. TC-1A: Open Sky with PPP and IMU

By reducing the URA to 20 cm and satellite nominal bias (B_{nom}) to 10 cm, as a result of the correction from the HAS, combined with the PL propagation from the IMU and Kalman filter, the following simulation results are obtained (see Figure 2). The availability map below is the result for the open-sky scenario, where a VAL of 30 m and HAL of 20 m was applied with the original P_{sat} and P_{const} values (From stakeholder interviews, the requirements have been determined for operational scenarios such as U-Space, geofencing and search and rescue. In open sky, these operations require an accuracy of 10 m (1 m in

urban environment), 95% availability (99.5% in urban), a continuity of 10^{-5}/hour, integrity risk of 10^{-7}, time-to-alert of 6 s and alert limits of 20 m horizontally and 30 m vertically). As can be seen, most of the globe exceeds 99.9% availability. In fact, the 95% availability is reached for the entire volume simulated. Without the need for integrity commitment by HAS, the open sky requirements for integrity can therefore be reached.

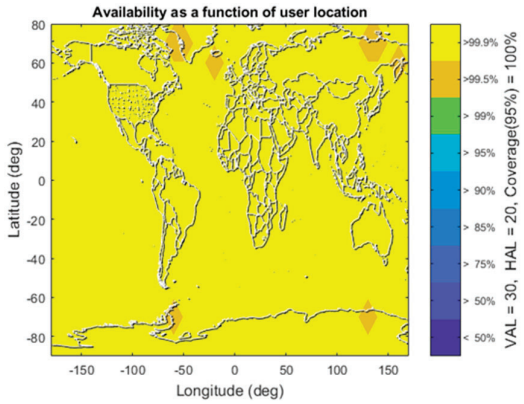

Figure 2. Open sky with PPP and IMU availability map indicating 95% values.

4.1.2. TC-1B: Open Sky with IMU and without PPP

In case of an HAS outage (URA = 2 m (GPS) 6 m (GAL), bnom = 0.75 m), or when other reasons not to apply the PPP corrections exist, the performance of the ARAIM-based integrity determination will decrease. This is a result of the deteriorating accuracy, whereas the number of visible satellites does not differ. It can be seen in Figure 3, that the AL requirements cannot be met and the availability is close to 0%. The best performance is achieved around the equator, but it is still significantly below the required 95% availability threshold.

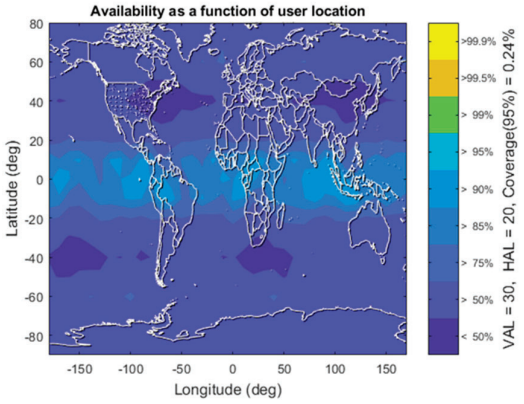

Figure 3. Open sky with IMU and without PPP availability map indicating 95% values.

4.1.3. TC-1C: Urban with PPP and IMU

In this test, an urban scenario with buildings blocking the horizon has been applied to determine the multipath, masking and non-line-of-sight signals. This scenario, based on the Schuman Roundabout in Brussels, has been applied to all the different grid locations.

The result of this simulation can be found in Figure 4. Here, a latitude effect becomes visible due to the orientation of the simulated building masks, which has a different obstruction in the northern direction as it has from the southern. The number of satellites visible is therefore lower in the European service area; this is completely dependent on the building geometry and orientation.

As a result of the poor conditions, the protection levels have increased with respect to the urban scenario and the availability has degraded.

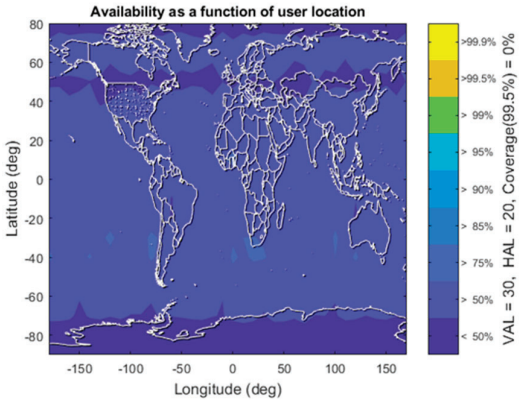

Figure 4. Urban with PPP and IMU availability map indicating 95% values.

4.1.4. TC-1D: Suburban with PPP and IMU

In the previous tests, UAV operations in open-sky and (deep) urban conditions have been evaluated. For this scenario, a set of parameters is modified with respect to the open-sky and urban conditions. The same elevation mask is used as for the urban scenario (Schuman Roundabout), but now with only a third of the signals being blocked. This approach is chosen to remove the bias from selecting a specific azimuth range for which signals are blocked and the impact this has on the geometry and GDOP. Furthermore, an elevation mask of 5 degrees is applied to remove the influence of low elevation satellite signal distortions. The multipath model is chosen in between that of open-sky and urban environments, as obtained from previous work [7].

The results of the simulation with these settings can be found in Figure 5, where the availability is displayed with coverage metrics.

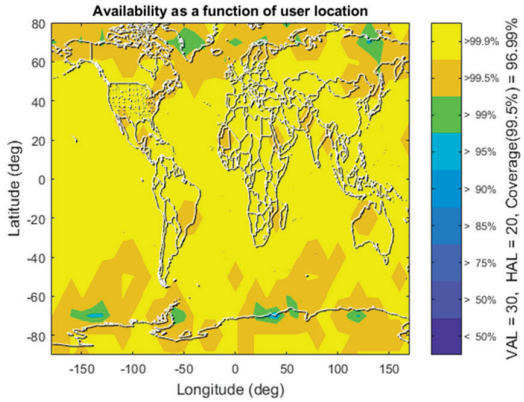

Figure 5. Suburban with PPP and IMU availability map indicating 95% values.

Without the need for integrity commitment, i.e., reduced satellite and constellation prior fault probabilities, as well as further accuracy improvements, the availability requirement is achieved for most of the service volume. Only at some high (70 degrees) latitudes, further improvements are required. At these locations, the suburban assumption is questionable, however, and open-sky performance is more likely. Therefore, the displayed results were deemed satisfactory and no further parameter assessment was performed.

Some remarks have to be stated regarding these results, however. First of all, as the number of available satellites with a direct line of sight is critical to the displayed results, the signal mask and building or environment model has a big influence on the results. Depending on the user location, these parameters may change resulting in significant variations in the availability. However, the results displayed here are a strong indicator that the proposed ARAIM evolution allows for use of UAVs in suburban environments.

4.2. Test Case 2

The influence of the feared events is best tested with the protection levels provided by the ARAIM algorithm under urban settings. The results are shown in Figure 6, the horizontal error and protection levels are displayed on the left, while the right hand side figure outlines the results in the vertical direction. In grey, the five distinct feared event scenarios are overlaid, matching the protection level increments. The dashed line is an indicator of the alert limit; the protection levels should remain below this threshold for the availability of the algorithm. The error with respect to the 'truth track', the combined forward and backward solution of the open sky (i.e., without feared events), is displayed in blue. The red dots display the results of the protection level outputted by the snapshot ARAIM algorithm modified with the settings just described. After propagation with the Kalman filter, the results in yellow are obtained.

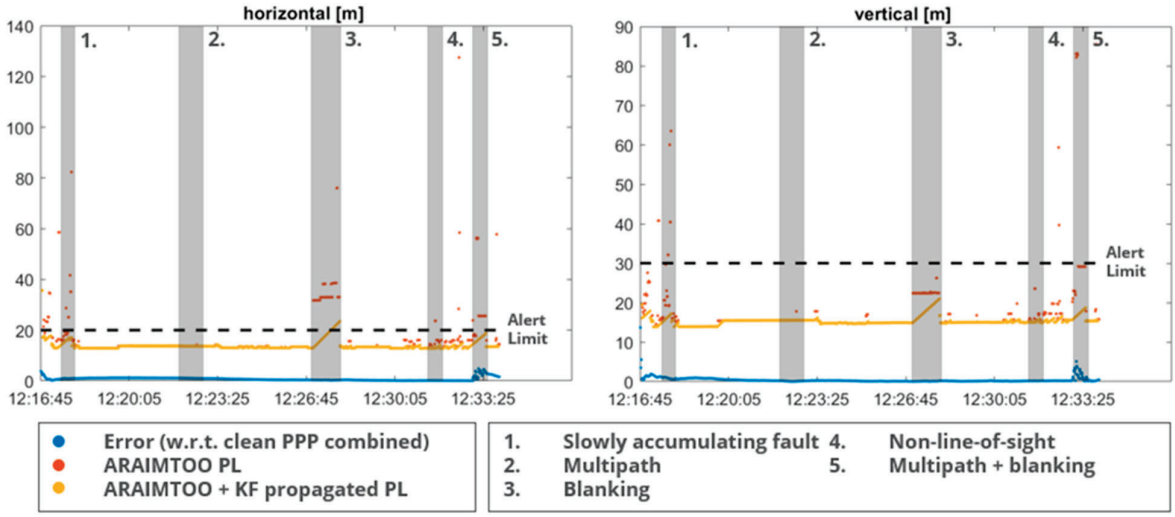

Figure 6. Protection level and positioning error for the urban UAV scenario.

Starting with the most significant impact visible, the protection level is severely impacted by the number of satellites visible due to blanking (indicated by the grey Sections 3 and 5). Even though the snapshot algorithm causes the horizontal protection level to exceed the alert limit immediately, the fusion with the IMU data allows for an extended duration of the availability. Such behavior allows for instance availability while moving through an underpass or through deep urban canyons for short durations. After roughly 45 s (during feared event 3), the alert limit is exceeded, which is a duration depending on the specifications of the IMU and implementation of the Kalman filter. Furthermore, it is interesting to note that especially during feared event 3, the actual error with respect to the open-sky 'truth track' is very small. This indicates there is more room for algorithm improvement in both the calculation of the protection level, for instance with tighter bounding, as well as the propagation algorithm.

Another interesting observation is made with the help of the RTKLib output, which is used for post-processing the data with PPP [8]. During the slowly accumulating fault period, the built-in checks already provide FDE functionality, which means not all introduced fault are observed in these results.

5. Conclusions

The proposed solution provides the following advantage, over stand-alone GNSS (using legacy ARAIM)

- A higher accuracy through HAS/PPP processing in combination with hybridization through filtering techniques, including IMU data.

- A reduced vulnerability to local disturbances such as multipaths in the urban environment. This results in a higher availability and continuity of service.
- Tighter integrity budgets and protection level bounding through reduced p_{sat}, p_{const} and b_{nom}, as well as added p_{nonlos} and $p_{cycleslip}$. This is further enabled through the comparison of the protection level calculated by ARAIM and the propagated state.
- More robust to GNSS outages due to hybridization with IMU.
- An improved FDE through residual monitoring within the Kalman filter.
- An improved time-to-alert due to filtering techniques leveraging the IMU information.

5.1. Conclusions from Service Volume Simulations

The combination of the GNSS dual frequency dual constellation measurements, with PPP processing based on the High Accuracy Service and hybridized with IMU measurements, results in ARAIM's eligibility for the open-sky UAV user sector. The significant reduction in, amongst others, the URA and the improvement in the available satellites with respect to the legacy ARAIM implementation for aviation, results in reduced protection levels over the globe. Reducing the URA significantly should be analyzed further for its consequences, as this could affect the P_{sat} and P_{const} values. It might be more feasible to reduce the URE instead, but this is beyond the scope of the presented work. Without PPP, the accuracy required for open-sky applications cannot be met, and other means of accuracy improvement have to be applied.

For UAV operations in the urban environment, the baseline settings considered do not result in acceptable availability. When considering the lower fault probabilities of both the satellite and constellation, the results are on the border of providing adequate availability. In the European service area, the requirements can be met with such settings. Although HAS does not commit on integrity, there is room for a discussion on implementing such values, especially considering the extra fault detection capabilities that the Kalman filter offers.

For global acceptance, also outside the European service area, some further improvements have to be considered. The improvement of the tropospheric variance due to PPP processing, as well as the reduced URA to 10 cm do not provide enough improvement. It should be noted that, since most of the area does not meet the availability requirements, the urban scenario may not be appropriate. For instance, better performance over the ocean could be expected, thereby closing in on the global availability requirement.

5.2. Conclusions on Feared Events Performance

The added benefit of hybridizing the ARAIM algorithm with PPP input and IMU data is clear. A significant improvement in the accuracy and integrity bounding is obtained.

6. Discussion and Recommendation

The proposed ARAIM evolution exceeds the 95% availability required for open-sky flights. This would allow, for example, for geo-referencing, drone operation under U-space, and search and rescue applications in open-sky settings. When considering UAV applications in the suburban environment, no further developments are required to meet the availability requirements. It should be noted, as the line between suburban and urban is blurred, thorough further studies with real flight data are required, evaluating the settings and assumptions applied in this chapter. It should be noted that the assumptions made in this work are very conservative. Some of the assumptions could be relaxed in a future analysis.

An even better performance could be achieved by further developing the following points:

- The use of more than two constellations will increase the satellite availability and therefore decrease the protection levels.
- A longer duration of the availability during lower satellite visibility can be achieved with further improved Kalman filter implementations.
- A longer duration of the availability during lower satellite visibility can be achieved with higher-grade IMUs.

- Tighter ARAIM budgets are possible, considering the propagation mitigates outages and rapid variations in the calculated PL.
- The further enhancement of PPP can result in lower protection levels which are more in line with the actual positioning error after filtering.

And, most importantly, further analysis of flight data is required to test under actual urban conditions. Statistically significant conclusions require multiple flights to be recorded, such as those displayed here, which requires a proper amount of testing.

Author Contributions: M.S. (Merle Snijders) and H.E. were responsible for the design and testing of the ARAIM evolution for unmanned aerial vehicles. E.D., G.M., F.B., J.M. and J.P.D. were responsible for the other sectors (rail and maritime) in the project and J.F. led the project. The EC (I.M., M.S. (Matteo Sgiammini) and J.P.B.) provided guidance, funding and reviewing. All authors have read and agreed to the published version of the manuscript.

Funding: The work is performed in the frame of the ARAIMTOO (ARAIM for Applications Beyond the Aviation Sector) project, funded by the EC (European Commission) as part of the Horizon 2020 R&D Programme and aimed at studying the use of ARAIM in sectors beyond aviation. The project's consortium is led by GMV, with VVA and NLR as partners.

Institutional Review Board Statement: Not applicable.

Informed Consent Statement: Not applicable.

Data Availability Statement: Data sharing is not applicable to this article.

Conflicts of Interest: The authors declare that this study received funding from the European Commission. The funder had the following involvement with the study; guidance and reviewing.

References

1. Precedence Research. *Unmanned Aerial Vehicle (UAV) Market (By Class: Tactical UAVs, Small UAVs, and Strategic UAVs; By Technology: Fully-Autonomous, Semi-Autonomous, and Remotely Operated; By System: UAV Payloads, UAV Airframe, UAV Avionics, UAV Software, and UAV Propulsion; By Application: Commercial, Military, and Recreational)-Global Industry Analysis, Size, Share, Growth, Trends Analysis, Regional Outlook and Forecasts, 2021–2030. Report Code 1269*; Precedence Research Pvt. Ltd.: Ottawa, ON, Canada, 2020.
2. Isik, O.K.; Hong, J.; Petrunin, I.; Tsourdos, A. Integrity analysis for GPS-based navigation of UAVs in urban environment. *Robotics* **2020**, *9*, 66. [CrossRef]
3. Fidalgo, J.; Domínguez, E.; Moreno, G.; Buendía, F.; Duque, J.P.; Martínez, J.; Snijders, M.; Engwerda, H.; Burdash, O.; Luciano, A.; et al. ARAIM for Applications Beyond Aviation. In Proceedings of the 35th International Technical Meeting of the Satellite Division of The Institute of Navigation, ION GNSS+ 2022, Denver, CO, USA, 19–23 September 2022; pp. 725–751.
4. Jan, S.-S.; Chan, W.; Walter, T.; Enge, P. Matlab simulation toolset for SBAS availability analysis. In Proceedings of the 14th International Technical Meeting of the Satellite Division of The Institute of Navigation (ION GPS 2001), Salt Lake City, UT, USA, 11–14 September 2001; pp. 2366–2375.
5. WG-C Advanced RAIM Technical Subgroup Reference Airborne Algorithm Description Document. 2017. Available online: https://web.stanford.edu/group/scpnt/gpslab/website_files/maast/ARAIM_TSG_Reference_ADD_v3.0.pdf (accessed on 19 December 2021).
6. Kaplan, E.D.; Hegarty, C. (Eds.) *Understanding GPS/GNSS: Principles and Applications*; Artech House: New York, NY, USA, 2017.
7. Martini, I.; Susi, M.; Paonni, M.; Sgammini, M.; Fernandez-Hernandez, I. Satellite Anomaly Detection with PPP Corrections: A Case Study with Galileo's High Accuracy Service. In Proceedings of the 2022 International Technical Meeting of The Institute of Navigation, Long Beach, CA, USA, 25–27 January 2022; pp. 1246–1262.
8. Takasu, T.; Yasuda, A. Development of the low-cost RTK-GPS receiver with an open source program package RTKLIB. In Proceedings of the International Symposium on GPS/GNSS, Seogwipo-si, Republic of Korea, 4–6 November 2009; Volume 1, pp. 1–6.